

An enhanced multi-objective differential evolution algorithm for dynamic environmental economic dispatch of power system with wind power

Yingjie Bai  | Xuedong Wu | Aiming Xia

School of Electronics and Information,
Jiangsu University of Science and
Technology, Zhenjiang, China

Correspondence

Xuedong Wu, School of Electronics and
Information, Jiangsu University of Science
and Technology, Zhenjiang, Jiangsu
212003, China.
Email: woolcn@163.com

Funding information

Postgraduate Research & Practice
Innovation Program of Jiangsu Province,
Grant/Award Number: KYCX20_3145

Abstract

Dynamic environmental economic dispatch (DEED) with wind power is an important extension of the classical environmental economic dispatch (EED) problem, which could provide reasonable scheduling scheme to minimize the pollution emission and economic cost at the same time. In this study, the combined dynamic scheduling of thermal power and wind power is carried out with pollutant emission and economic cost as optimization objectives; meanwhile, the valve-point effect, power balance, ramp rate, and other constraints are taken into consideration. In order to solve the DEED problem, an enhanced multi-objective differential evolution algorithm (EMODE) is proposed, which adopts the superiority of feasible solution (SF) and nondominated sorting (NDS) two selection strategies to improve the optimization effect. The suggested algorithm combines the total constraint violation and penalty function to deal with various constraints, due to different constraint techniques could be effective during different stages of searching process, and this method could ensure that each individual in the Pareto front (PF) is feasible. The results show that the proposed algorithm can deal with DEED problem with wind power effectively, and provide better dynamic scheduling scheme for power system.

KEYWORDS

dynamic environmental economic dispatch, enhanced multi-objective differential evolution algorithm, selection strategies, wind power

1 | INTRODUCTION

The EED problem has attracted more and more attention of researchers because of global warming, greenhouse efficiency, and other issues, which could provide reasonable dispatching scheme to save the economic cost and improve the environmental pollution.¹ DEED is an important part of EED, which is a nonlinear, strongly constrained, high-dimensional

multi-objective optimization problem. DEED takes ramp rate constraint into consideration, which is not considered in EED,^{2,3} and DEED needs to minimize two conflicting objective functions (cost and emission) while satisfying various constraints.⁴ Thus, the DEED problem becomes more difficult to solve, and many researchers are committed to finding a better algorithm for solving this problem and have done a lot of work.⁴ At present, the solving methods of DEED can

This is an open access article under the terms of the Creative Commons Attribution License, which permits use, distribution and reproduction in any medium, provided the original work is properly cited.

© 2020 The Authors. *Energy Science & Engineering* published by the Society of Chemical Industry and John Wiley & Sons Ltd.

be classified into two groups: deterministic-based techniques and heuristic-based techniques.^{5,6}

For deterministic-based techniques, the optimization objectives are usually combined linearly with the given objective weight, and the DEED problem is transformed into a single-objective optimization problem.^{7,8} Basu⁹ proposed a particle swarm optimization (PSO) algorithm to deal with the DEED problem, and the two optimization objectives are combined with liner-weighted method linearly. Considering the valve-point effect, Hemamalini et al¹⁰ presented a Maclaurin series-based Lagrangian method to solve the dynamic economic dispatch problem. Arul et al¹¹ suggested three kind of differential harmony search algorithms by transforming the multi-objective into a single objective, in which the objective weight changed with step and each step would produce an optimal compromise solution. Although these methods improve the optimization mechanism and can achieve certain successful results, there are still some defects: (a) They may fall into local optimization and result in premature convergence of the problem easily; (b) it is difficult to determine the target weight in practice.^{12,13}

For heuristic-based techniques, the DEED problem is treated as real multi-objective optimization problem. The multi-objective optimization evolution algorithm (MOEA) can avoid the defects of weighted sum methods in solving the DEED problem.¹⁴ Basu¹⁵ took the DEED problem as the true multi-objective optimization problem with nondominated sorting genetic algorithm-II (NSGA II), and obtained the PF (the set of optimal solutions) of DEED problem for the first time. Guo et al¹⁶ presented a new MOEA algorithm which used group search optimizer with multiple producers to solve the DEED problem, and this algorithm could get better PF than the NSGA II. For decision-making, a technique for order preference similar to an ideal solution was developed as well in Ref. 16 Using niche technology to allocate search resources reasonably, Niknam et al¹⁷ suggested a θ -multi-objective teaching-learning-based optimization algorithm for the present problem and the optimization process of the algorithm was improved. Roy et al¹⁸ proposed a hybrid differential evolution-based chemical reaction optimization (HCRO) algorithm for the nonlinear DEED problem, which could improve the quality and convergence speed of the solution. Huang et al¹⁹ considered the power generation limit and developed a new algorithm, which named simplified swarm optimization-differential evolution and sequential quadratic programming algorithm (SSO-DE-SQP), this method had great power in dealing with the large-size DEED problem. Compared with the single-objective optimization algorithms, these multi-objective optimization algorithms are better in solving the DEED problem. However, it is still the research focus to find a better optimization algorithm to reduce environmental pollution and save economic cost.²⁰

Usually, many algorithms for solving the DEED problem contain only one selection strategy, and some high-quality individuals are selected according to the criteria of the strategy in each generation population, so the target space cannot be fully explored. In order to search the target space to a greater extent, this paper develops an enhanced multi-objective differential evolution algorithm of DEED problem, which contains SF and NDS.^{15,21} Different selection strategies have different selection criteria, and the proposed algorithm randomly selects a selection strategy in each generation population to obtain some high-quality individuals, so it can ensure the diversity of individuals and expand the search range.^{22,23} Due to the influence of the proportion of feasible region and total space, the characteristics of the problem itself, and the search process, different methods could be effective in different solving stages,^{24,25} the suggested algorithm integrates two constraint processing techniques: penalty function and total constraint violation, and these techniques could ensure that only feasible individuals can be retained during the iteration process. In addition, this work takes fuzzy decision-making to get the best compromise solution from the PF obtained by the developed algorithm.^{26,27} This study takes the test system with and without wind power for simulation test, and the results show that the proposed algorithm is feasible and superior in dealing with the DEED problem, which can provide better dynamic scheduling scheme for decision-makers.

The rest of this paper is organized in following manner. Section 2 is the problem formulation. The suggested algorithm is elaborated in section 3. The simulation results and analysis are presented in section 4. The last section is the conclusion.

2 | PROBLEM FORMULATION

In this section, the mathematical models of economy and emission are proposed at first. Then, all equality and inequality constraints are taken into consideration. In addition, the handling technique for power balance constraints and ramp rate constraint is introduced.

2.1 | Economic cost

Economic cost is mainly divided into two parts: thermal power cost and wind power cost. Thermal power cost is mainly the cost of fossil fuel for thermal power generation. When the valve-point effect is considered, the cost function can be expressed as²⁸

$$F_{\text{ther}} = \sum_{t=1}^T \sum_{i=1}^N a_i + b_i P_{i,t} + c_i P_{i,t}^2 + \left| d_i \sin(e_i (P_{i,\min} - P_{i,t})) \right| \quad (1)$$

where N is the number of thermal power units, T is the entire scheduling cycle, $P_{i,t}$ is the power output of i^{th} thermal unit at time period t , $P_{i,\min}$ is the lower power limit of i^{th} thermal unit, and a_i, b_i, c_i, d_i, e_i are fuel cost coefficients of the i^{th} thermal unit, they could be found from Table A1 of the appendix.

The direct cost coefficient of wind power C_w is introduced in the present work, and the direct cost of wind power is related to power generation. Their relationship could be described as

$$F_{\text{wind}} = \sum_{t=1}^T C_w \times P_{w,t} \quad (2)$$

where $P_{w,t}$ is the wind power output at time period t .

According to the Equations 1 and 2, the total economic cost is

$$F_{\text{total}} = F_{\text{ther}} + F_{\text{wind}} \quad (3)$$

2.2 | Pollution emission

Pollution emission, which is related to the power generation of thermal power, is mainly generated by fossil fuel combustion in thermal power generation, and the optimization objective of emission can be expressed as¹⁵

$$E = \sum_{t=1}^T \sum_{i=1}^N \alpha_i + \beta_i P_{i,t} + \gamma_i P_{i,t}^2 + \delta_i \exp(\mu_i P_{i,t}) \quad (4)$$

where $\alpha_i, \beta_i, \gamma_i, \delta_i,$ and μ_i are emission curve coefficients of the i^{th} thermal unit, they are given in Table A2 of the appendix.

2.3 | Operational constraints and processing method

2.3.1 | Power balance constraint

The power balance constraint is an equality constraint, which can be expressed as

$$\sum_{i=1}^N P_{(i,t)} + P_{(w,t)} - P_{(D,t)} - P_{(L,t)} = 0 \quad t = 1, 2, \dots, T \quad (5)$$

where $P_{w,t}$ is wind power output at time period t , $P_{D,t}$ is the total demand at time period t , and $P_{L,t}$ is the system loss which can be obtained by B-coefficients method.

For the power balance constraint, the constraint violations are calculated in each scheduling period and the output of each unit is adjusted in real time. For t period, set a maximum

adjustment number, the constraint violation of t period is calculated as

$$\Delta P_t = P_{D,t} + P_{w,t} + P_{L,t} - \sum_{i=1}^N P_{i,t} \quad (6)$$

If ΔP_t is less than threshold ϑ , then no adjustment is required, else $P_{i,t}$ will adjust as

$$P_{i,t} = P_{i,t} + \frac{\Delta P_t}{N} \quad i = 1, 2, \dots, N \quad (7)$$

Although the output of each unit has been adjusted K times for a certain individual at t period, it may still not meet power balance constraint condition. In the subsequent operation, it is still necessary to calculate the violation degree of power balance constraint for the modified individual.

2.3.2 | Power upper and lower limit constraint

During the operation of the system, the actual power of all thermal power units must be within the feasible range and shall not be operated with low power, or overload.

$$P_{i,\min} \leq P_{i,t} \leq P_{i,\max} \quad (8)$$

where $P_{i,\min}$ and $P_{i,\max}$ are upper and lower limits of the i^{th} output unit in the dispatch period, they are shown in Table A1 of the appendix.

2.3.3 | Ramp rate constraint

Between different dispatching periods, the actual output of the unit needs to be adjusted. In the regulation process, the regulation capacity of each unit in a short period of time should be considered, which is limited by climbing constraints.²⁹

$$\begin{cases} P_{i,t} - P_{i,t-1} - U_{Ri} \times \Delta T \leq 0 \\ P_{i,t-1} - P_{i,t} - D_{Ri} \times \Delta T \leq 0 \end{cases} \quad i = 1, \dots, N \quad (9)$$

where ΔT is scheduling interval, U_{Ri} and D_{Ri} are up and down ramp constraints of i^{th} unit.

The variable dimension of dynamic dispatch is high and serious coupling between variables. In addition to the unit output adjustment mentioned above, the climbing constraint will be handled in the following way.

For different dispatching periods, the output upper and lower limits of thermal power units are

$$\left\{ \begin{array}{l} P_{i,t,min} = \begin{cases} P_{i,min} & t=1 \\ \max(P_{i,min}, P_{i,t-1} - D_{Ri}) & \text{otherwise} \end{cases} \\ P_{i,t,max} = \begin{cases} P_{i,max} & t=1 \\ \min(P_{i,max}, P_{i,t-1} + U_{Ri}) & \text{otherwise} \end{cases} \end{array} \right. \quad (10)$$

Then, the adjusted output unit is

$$P_{i,t} = \begin{cases} P_{i,t,min} & P_{i,t} < P_{i,t,min} \\ P_{i,t} & P_{i,t,min} \leq P_{i,t} \leq P_{i,t,max} \\ P_{i,t,max} & P_{i,t} > P_{i,t,max} \end{cases} \quad (11)$$

2.3.4 | System up and down spinning reserve capacity constraint

Up spinning reserve capacity constraint:

$$P_{w,t} \times w_u\% + P_{D,t} \times L\% - \sum_{i=1}^N U_{i,t} \leq 0 \quad (12)$$

$$U_{i,t} = \min(U_{Ri} \times T_{10}, P_{i,max}) \quad (13)$$

Down spinning reserve capacity constraint:

$$(P_{w,max} - P_{w,t}) \times w_d\% - \sum_{i=1}^N D_{i,t} \leq 0 \quad (14)$$

$$D_{i,t} = \min(D_{Ri} \times T_{10}, P_{i,t} - P_{i,min}) \quad (15)$$

where $w_u\%$ is wind power prediction error at time period t , $L\%$ is the demand coefficient of system load forecasting error of up spinning reserve, $P_{w,max}$ is the rated power of wind power, $w_d\%$ is the demand coefficient of down spinning reserve caused by wind power prediction error, and T_{10} is the response time of spinning reserve.

2.4 | Constraint multi-objective optimization problem

The DEED problem can be formulated as

$$\text{Min } F(x) = \{ \min[F_{\text{total}}(x)], \min[E(x)] \} \quad (16)$$

$$\text{Subject to: } \begin{cases} g_i(x) = 0 & i = 1, 2, \dots, G \\ h_j(x) \leq 0 & j = 1, 2, \dots, H \end{cases} \quad (17)$$

where $F_{\text{total}}(x)$ and $E(x)$ are the optimization objectives, and $g_i(x)$ and $h_j(x)$ are equality and inequality constraints.

3 | THE PROPOSED SOLVING METHOD FOR DEED

3.1 | EMODE algorithm

Differential evolution (DE) algorithm has strong ability for solving single-objective problem, which is extended into a multi-objective evolution algorithm for DEED in present study. The proposed EMODE algorithm combined two selection strategies based on DE, and the constraint processing technique of each strategy is different, which could make full use of the advantages of these two strategies.

Differential evolution starts with an initial population Ω generated randomly, and the population size is N_p . The initial population is generated as¹¹

$$x_\varphi = x_{\min} + \text{rand}(x_{\max} - x_{\min}) \quad (18)$$

where x_φ is a random individual of the population, and x_{\min} and x_{\max} are the upper and lower limits of each individual. The encoded individual can be described as

$$x_\varphi = \begin{bmatrix} \varepsilon_{11} & \varepsilon_{12} & \dots & \varepsilon_{1N} \\ \varepsilon_{21} & \varepsilon_{22} & \dots & \varepsilon_{2N} \\ \vdots & \vdots & \ddots & \vdots \\ \varepsilon_{T1} & \varepsilon_{T2} & \dots & \varepsilon_{NT} \end{bmatrix} \quad (19)$$

where N is the number of thermal units and T is total scheduling period.

Mutation and crossover are two important parts of DE algorithm. During the process of mutation, a mutation vector u_φ is generated by mutation operator for individual x_φ in the population. Mutation vectors are generated as

$$u_\varphi = x_\varphi + F_{\text{muta}}(x_\varphi - x_\rho) \quad (20)$$

Where x_φ , x_ρ , and x_ρ are three individuals randomly selected from the population $P(\varphi \neq \varpi \neq \rho \neq \varphi)$, and F_{muta} is the mutation parameter to control the disturbance of variation.

For the process of crossover, the corresponding components between x_φ and u_φ are selected by crossover operator to generate a trial vector v_φ . The test vector is generated as.

$$v_{\varphi,j} = \begin{cases} u_{\varphi,j}, & \text{if } r \text{ and } j \leq C_R \text{ or } j = q \\ x_{\varphi,j}, & \text{otherwise} \end{cases} \quad (21)$$

where r and j is a random number subject to uniform distribution between $[0,1]$, C_R is cross parameter, which used to control the diversity of population and avoid the algorithm falling into local optimum, parameter q can avoid the individual $v_{\varphi,j}$ to be the same as the previous individual $x_{\varphi,j}$.

EMODE algorithm modifies the selection strategy of traditional DE and includes two selection sections: SF and NDS. For each iteration, a random number r and s between $[0,1]$ will be generated when the present algorithm performs the selection operation. If r and s is less than 0.5, NDS will be used for selection operation, else SF will be selected.

- If NDS is chosen, the algorithm performs nondominated sorting and congestion calculation for each individual, and all constraints will be processed by penalty function. The total constraint is calculated as

$$V(x) = \sum_{t=1}^T \left| \sum_{i=1}^N P_{i,t} + P_{w,t} - P_{D,t} - P_{L,t} \right| + \sum_{t=1}^T \max \left[\left(P_{w,t} \times w_u \% + P_{D,t} \times L \% - \sum_{i=1}^N U_{i,t} \right), 0 \right] + \sum_{t=1}^T \max \left[\left(P_{w,max} - P_{w,t} \right) \times w_d \% - \sum_{i=1}^N D_{i,t}, 0 \right] \quad (22)$$

The optimization objective function will be transformed into the following form

$$F(x) = F(x) + \rho V(x) \quad (23)$$

where ρ is a penalty coefficient.

- If SF method is adopted, the constraint of each individual will be reflected by the total constraint violation³⁰

$$\varepsilon(x) = \frac{\sum_{k=1}^{N_c} u_k T_k(x)}{\sum_{k=1}^{N_c} u_k} \quad (24)$$

where $T_{k,max}$ is the obtained maximum violation of constraint $T_k(x)$ so far and $u_k = 1/T_{k,max}$, N_c is the number of constraints.

In the process of solving, the total constraint violation is used to judge whether each individual is a feasible individual.

All individuals in the population are subject to the following criteria (η and ζ are individuals in the population).

- η and ζ are feasible, and η has better objective function value than ζ , then η is superior to ζ ;
- η is feasible and ζ is infeasible, then η is superior to ζ ;
- η and ζ are infeasible, and η has smaller total constraint violation, then η is superior to ζ .

In Condition 1, only the objective function values are compared between two feasible individuals, which could improve the quality of the overall population, so only the feasible individuals with optimal objective function values would be selected. In Condition 2, feasible individuals are always considered superior to infeasible individuals, so feasible ones would be selected. In Condition 3, only the total condition violations are compared between two infeasible individuals, which could make the infeasible individuals fly to the feasible region, so only the infeasible individuals with low total constraint violations would be selected.²⁴

3.2 | Fuzzy decision-making technique

A group of Pareto optimal solutions can be obtained through the algorithm in this paper. However, from the practical point of view, the decision-maker needs to evaluate the scheduling results comprehensively according to the trade-off between scheduling objectives and subjective preference information, and select a feasible optimal compromise solution. In essence, the decision-maker's judgment is difficult to quantify and describe accurately, so we consider to use the fuzziness of human decision-making to improve the decision-making effect by fuzzing the value of alternatives or the weight of decision-making experts in charge.

Fuzzy decision-making technique is used in our work to get the best compromise solution^{31,32}

$$\mu_{\xi}^m = \begin{cases} 1, & f_{\xi}^m \leq f_{\xi}^{m,min} \\ \frac{f_{\xi}^{m,max} - f_{\xi}^m}{f_{\xi}^{m,max} - f_{\xi}^{m,min}}, & f_{\xi}^{m,min} < f_{\xi}^m \leq f_{\xi}^{m,max} \\ 0, & f_{\xi}^m \geq f_{\xi}^{m,max} \end{cases} \quad (25)$$

where f_{ξ}^m is the m^{th} objective function value of the ξ^{th} optimal solution, N_{obj} is the number of objective functions, and $f_{\xi}^{m,max}$ and $f_{\xi}^{m,min}$ are maximum and minimum of the m^{th} objective function.

The satisfaction degree of each Pareto optimal solution is

$$\mu_{\xi} = \frac{\sum_{m=1}^{N_{obj}} \mu_{\xi}^m}{\sum_{\xi=1}^{N_t} \sum_{m=1}^{N_{obj}} \mu_{\xi}^m} \quad (26)$$

where N_t is the number of PF solution. The solution with the greatest satisfaction will be selected as the best compromise solution.

The computational steps of the proposed algorithm is shown in Procedure 1 below

Procedure 1. The procedure for solving the DEED problem based on EMODE

Step 1: Set algorithm parameters

G_{max} : total iterations; F_{muta} : mutation parameter; C_R : crossover parameter; N_p : size of the population; T : scheduling cycle; N : number of units.

Step 2: Initialize the population, $gen = 1$

Initialize the population according to Equation 8

$$x_{\varphi} = x_{min} + r \text{ and } (x_{max} - x_{min})$$

x_{min} and x_{max} are the upper and lower limits of thermal power units in this work.

Calculate the objective function value of each individual with constraint processing.

Step 3: Mutation

Generate N_p mutant individuals according to Equation 20

$$u_{\varphi} = x_{\sigma} + F_{muta} (x_{\phi} - x_{\sigma})$$

Step 4: Crossover

According to Equation 21, N_p test vectors are generated by comparing the target vector x_{φ} with the mutation vector u_{φ} :

$$v_{\varphi,j} = \begin{cases} u_{\varphi,j}, & \text{if } r \text{ and } j \leq C_R \text{ or } j = q \\ x_{\varphi,j}, & \text{otherwise} \end{cases}$$

Calculate the objective function value of each test individual under constraint processing.

Step 5: N_p test individuals are combined with the original population to form a new population with the size of $2N_p$.

Step 6: Selection

Generate a random number $rands$ between 0 and 1.

if r and $s < 0.5$

NDS is used for selection, and the individual constraint is dealt with penalty function. See Equations 22 and 23 for the specific method.

else

SF is used for selection. Select the appropriate individuals based on the conditions of SF which is shown in Section 3.1, and the total constraint violation is used to evaluate whether the individual is feasible, see Equation 24.

end

The select N_p high-quality individuals will be the parent population of the next generation.

Step 7: $gen = gen + 1$

If $gen < G_{max}$, go back to Step 3, otherwise go to Step 8.

Step 8: Output the best compromise solution with fuzzy decision-making technique according to Equations 25 and 26.

In step 6, if NDS is selected, all individuals are stratified according to the dominant relationship among individuals in the new population, and then, 100 high-quality individuals are selected in turn from the optimal layer down. Otherwise, the constraint violation degree of all individuals was

calculated, and then according to SF, the superiority among individuals was compared; finally, 100 superior individuals were selected.

In step 8, a PF composed of N_p optimal solutions is obtained by the proposed algorithm after G_{max} iterations, and then, the satisfaction degree of all individuals in the PF is calculated by fuzzy decision-making technique. The solution with the highest satisfaction degree is the best compromise solution.

4 | EXPERIMENTAL RESULTS AND ANALYSIS

To verify the effectiveness of the proposed algorithm, two kinds of simulation experiments are carried out in the cases of without wind power (case 1) and with wind power (case 2), and this work takes 24 hours as the dispatching cycle and one hour as the scheduling period.

For the simulation experiments of two cases, the population size N_p is 200, the scaling factor F_{muta} is 0.2, and the crossover probability C_R is 0.9. This work takes an i5-5200 U @2.20 GHz machine with 4 GB RAM for simulation test, and the software is MATLAB R2016b (64 bit).

The proposed algorithm is run 50 times under the same parameters, so out of 50 PFs. The best PF is selected by calculating the Hypervolume (HV) performance indicator of PFs with Hypervolume by Slicing Objectives (HSO) algorithm.³³ The advantage of HV indicator is that it takes diversity and convergence of the solutions into consideration at the same time. In practical multi-objective optimization problems, the dimension and numerical range of different objectives are different, so it is necessary to normalized the objectives. In this work, point (1,1) is used as a reference point to calculate the HV performance indicator of different PFs, and the PF with largest HV indicator is considered as the best PF. Table 1 shows the summary of HV indicator values of two cases study by using EMODE.

4.1 | Case 1

In this case, only simple thermal power dispatching is considered, and the simulation experiment of 10 units power system is carried out. The simulation results of the proposed algorithm are compared with others, which can verify the ability of the suggested algorithm to solve the

TABLE 1 HV indicator values of two cases with EMODE

Case no.	Min	Max	Mean
Case 1	0.8932	0.9106	0.9019
Case 2	0.9020	0.9302	0.9161

TABLE 2 Best compromise solution and extreme solution of different algorithms in case 1

Algorithm	Best economic		Best emission		Best compromise solution	
	Cost/ 10^6 \$	Emission/ 10^5 lb	Cost/ 10^6 \$	Emission/ 10^5 lb	Cost/ 10^6 \$	Emission/ 10^5 lb
NSGA II ¹⁵	2.5168	3.1740	2.6563	3.0412	2.5226	3.0994
RCGA ¹⁵	2.5268	3.1740	2.6563	3.0412	2.5251	3.1246
IBFA ³⁹	2.4818	3.2750	2.6143	2.9588	2.5171	2.9904
DE-SQP ³⁹	2.4659	-	-	-	2.4688	3.1564
PSO-SQP ³⁹	2.4668	-	-	-	2.4701	3.1507
MAMODE ²⁹	2.4925	3.1512	2.5816	2.9524	2.5141	3.0274
MODE ⁴⁰	2.5123	3.0113	2.5436	2.9639	5.5276	2.9805
MOHDE-SAT ⁴⁰	2.5080	3.0146	2.5470	2.9607	2.5279	2.9776
MOEA/D-DE	2.4802	3.1091	2.5700	2.9349	2.5146	2.9836
CRO ¹⁸	2.4816	2.9912	2.4836	2.9866	2.5178	3.0194
HCRO ¹⁸	2.4799	2.9874	2.4814	2.9846	2.5171	2.9907
BTLBO ⁴¹	2.4842	-	-	2.9481	2.5092	3.0306
ITLBO ⁴¹	2.4629	-	-	2.9185	2.5116	2.9837
EMODE	2.4910	3.0910	2.5560	2.9440	2.5110	2.9870

DEED problem. The detailed compared results are shown in Table 2, the best PF obtained by EMODE is shown in Figure 1, and the comparison of the best compromise solution is shown in Figure 2.

From Table 2, it can be seen that the best compromise solution of the developed algorithm is 2.511×10^6 \$ and 2.987×10^5 lb, which is better than many compared

algorithms. In terms of economy, the cost of the best compromise solution of the proposed algorithm is superior to NSGA II, RCGA, IBFA, MAMODE, IBFA, MODE, MOHDE-SAT, MOEA/D-DE, CRO, HCRO, and BTLBO. Compared with the MOHDE-SAT algorithm which has the lowest pollution emission among all these compromise solutions, the emission of the proposed algorithm is similar;

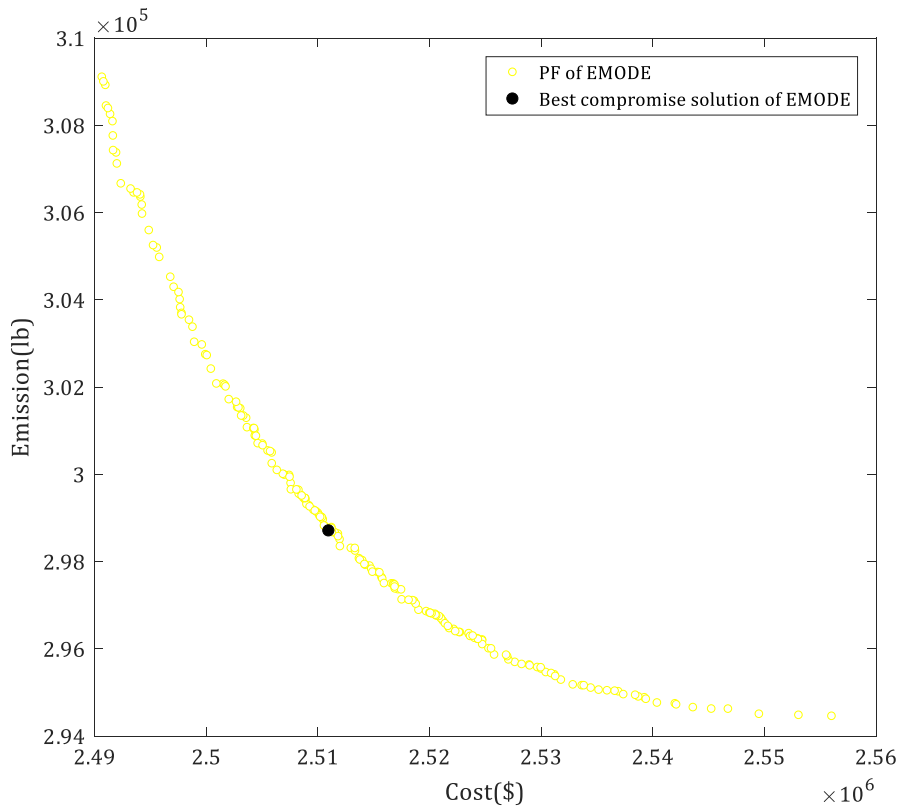
**FIGURE 1** PF obtained by EMODE in case 1

FIGURE 2 Comparison of optimal solutions in case 1

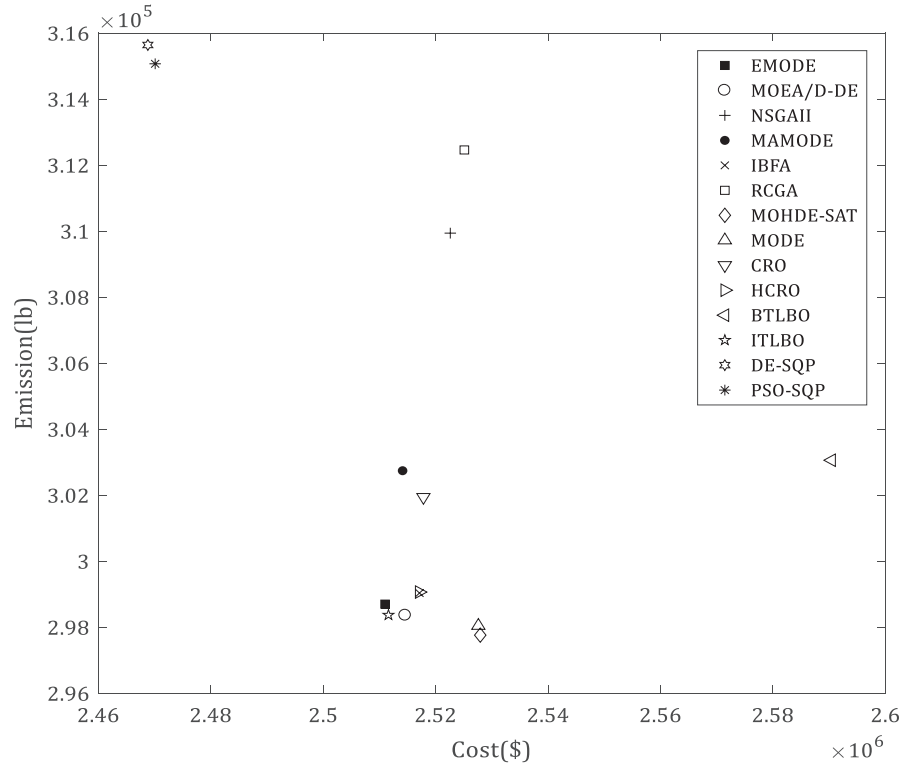


TABLE 3 Best compromise solution detail of the proposed algorithm in case 1

Time	Units output in each period/MW										Output/ MW	Loss/ MW	Load/ MW
	PG1	PG2	PG3	PG4	PG5	PG6	PG7	PG8	PG9	PG10			
1	150.00	135.00	96.60	96.33	136.33	126.29	99.50	96.74	70.79	48.05	1055.63	19.63	1036
2	150.40	135.41	105.80	117.02	173.70	137.95	99.81	98.57	68.69	44.99	1132.34	22.34	1110
3	226.37	137.62	121.02	128.94	166.98	145.82	112.22	116.52	77.34	54.68	1287.51	29.51	1258
4	224.80	147.26	155.67	169.80	210.87	159.56	127.05	117.41	76.55	53.49	1442.45	36.45	1406
5	226.86	143.52	184.83	196.00	226.75	159.41	129.96	118.69	80.00	54.27	1520.28	40.28	1480
6	227.51	197.78	228.75	236.36	242.19	159.86	129.80	119.80	80.00	55.00	1677.05	49.05	1628
7	227.04	238.96	262.68	239.57	243.00	160.00	129.94	120.00	79.88	54.96	1756.03	54.03	1702
8	226.69	284.57	276.17	260.21	242.99	156.00	129.96	119.99	79.99	54.80	1835.37	59.37	1776
9	303.74	294.81	309.01	299.41	243.00	160.00	130.00	120.00	80.00	55.00	1994.97	70.97	1924
10	375.00	309.19	331.18	299.66	242.87	159.89	129.79	119.89	79.90	54.55	2101.91	79.91	2022
11	381.34	384.61	340.00	299.98	242.99	159.99	123.00	119.99	79.98	54.99	2193.89	87.89	2106
12	403.85	411.14	339.82	299.88	242.98	159.93	129.98	119.99	79.98	54.95	2242.49	92.49	2150
13	379.27	349.88	339.92	299.80	242.97	160.00	129.96	119.99	79.82	54.94	2156.54	84.54	2072
14	303.63	301.17	314.47	287.91	242.98	159.97	129.99	119.99	79.97	54.96	1995.06	71.06	1924
15	303.83	252.72	248.36	243.97	243.00	159.99	130.00	120.00	79.31	54.93	1836.11	60.11	1776
16	227.17	198.24	194.88	213.25	224.74	159.44	128.22	119.14	78.78	54.86	1598.75	44.75	1554
17	150.43	197.92	193.59	202.7	231.32	159.86	129.95	119.93	79.11	54.98	1519.83	39.83	1480
18	226.96	186.58	234.11	242.28	242.83	159.83	129.71	119.84	79.95	54.86	1676.96	48.96	1628
19	303.51	249.81	242.85	254.02	242.93	159.71	129.75	119.54	79.48	54.47	1836.07	60.07	1776
20	380.42	282.32	304.08	293.02	243.00	160.00	130.00	120.00	80.00	55.00	2047.84	75.84	1972
21	305.07	310.50	304.79	287.01	243.00	160.00	130.00	119.83	80.00	55.00	1995.19	71.19	1924
22	300.37	259.76	229.10	237.01	195.15	121.64	107.52	105.63	74.10	48.87	1679.14	51.14	1628
23	226.34	185.48	155.09	187.28	160.76	122.12	94.60	100.65	79.45	53.51	1365.28	33.28	1332
24	227.12	136.15	99.599	152.43	151.92	139.12	102.82	106.31	52.58	42.16	1210.21	26.21	1184

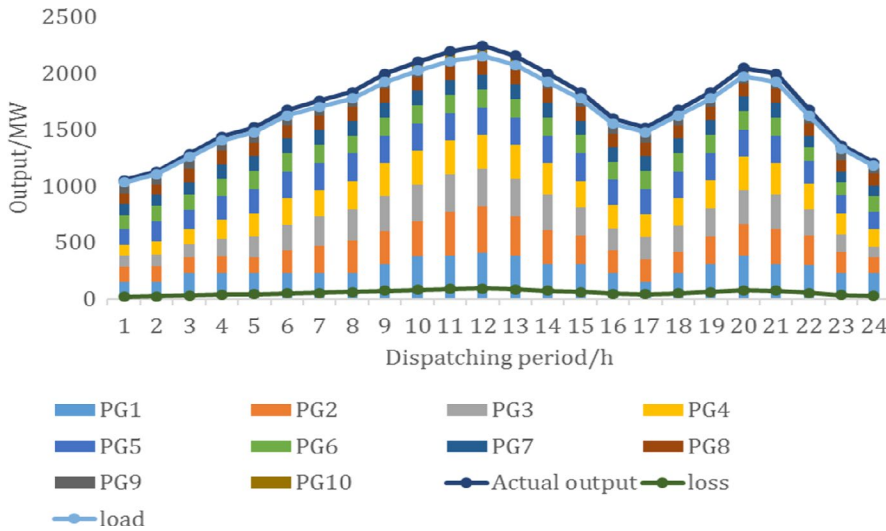


FIGURE 3 Power balance verification in case 1

meanwhile, EMODE saves 16 929\$ in economic cost. In terms of environment, the emission of the best compromise solution obtained by the developed algorithm is better than most of these compared algorithms, compared with DE-SQP, which reduces 16 940 lb pollution emission. In general, the solution of the proposed algorithm is superior to the comparison algorithms.

Figure 1 gives the PF of case 1 problem obtained by EMODE and the best compromise solution selected by fuzzy decision-making. The HV indicator of the present PF is 0.9106, which shows that the solutions in this PF have great diversity and convergence and that the proposed algorithm has great search ability. The comparison of the best compromise solutions obtained by different algorithms is shown in Figure 2, from which we can clearly see that the best compromise solution of EMODE is superior to most algorithms. Compared with ITLBO, the best compromise solution of EMODE is slightly insufficient in terms of pollution emissions, but can save more costs in terms of economic.

The details of the best compromise solution of EMODE are provided in Table 3, and the power balance is verified in Figure 3 graphically. Figure 3 shows that the constraint handling techniques adopted in EMODE have great effect on power balance constraint, and the optimal dispatch scheme could make the actual output of all units meet the load demand and network loss.

4.2 | Case 2

As a renewable energy, wind power has the advantages of clean, low cost and large installed capacity, and wind energy is never exhausted. Wind power can not only provide stable power supply for economic growth, but also effectively

alleviate air pollution, water pollution and global warming. In case 2, wind power is taken into consideration, and this case takes 10 thermal power units and 1 wind farm as dispatching objects.

When the wind power is connected to the grid, the wind farm with 50 wind turbines is connected to the 10-unit power system, in which the rated generating capacity of each wind turbine is 2 MW. The predicted output of the wind farm is shown in Figure 4. The dispatching results of power system with wind power, which obtained by EMODE, are compared with other three algorithms in detail, as shown in Table 4, and the PF obtained by the proposed algorithm is shown in Figure 5. Figure 6 is the verification result of power balance constraint, which can reflect the feasibility of the dispatch result to some extent, and the specific information of the best compromise solution is shown in Table 5.

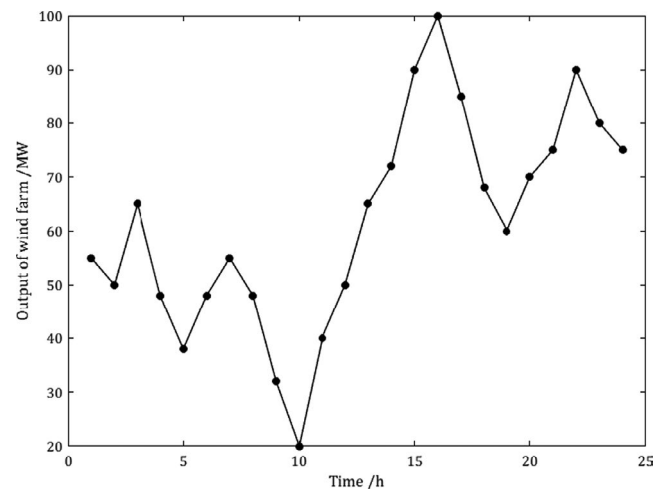


FIGURE 4 Forecast output of wind farm

TABLE 4 Best compromise solution and extreme solution of different algorithms in case 2

Algorithm	Best economic		Best emission		Best compromise solution	
	Cost/10 ⁶ \$	Emission/10 ⁵ lb	Cost/10 ⁶ \$	Emission/10 ⁵ lb	Cost/10 ⁶ \$	Emission/10 ⁵ lb
NSGA II	2.3777	2.7344	2.4101	2.6760	2.3923	2.7002
MOEA/D-DE	2.3598	2.8252	2.4541	2.6350	2.3870	2.6957
MODE-ESM	2.3547	2.8574	2.4347	2.6630	2.3919	2.6999
EMODE	2.3621	2.7362	2.4230	2.6350	2.3860	2.6525

FIGURE 5 PF and comparison of optimal solutions in case 2

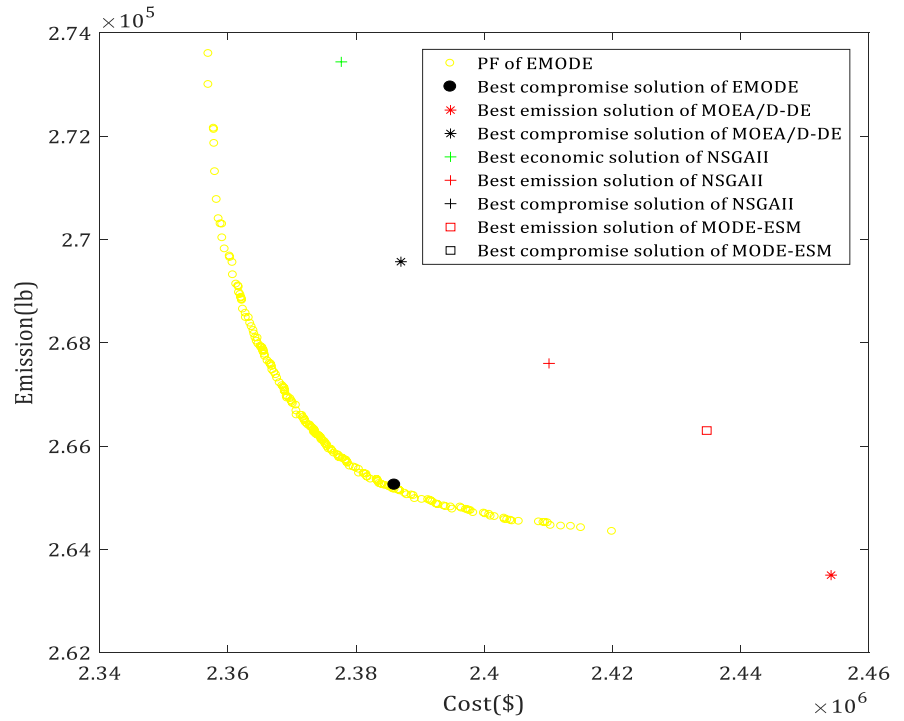
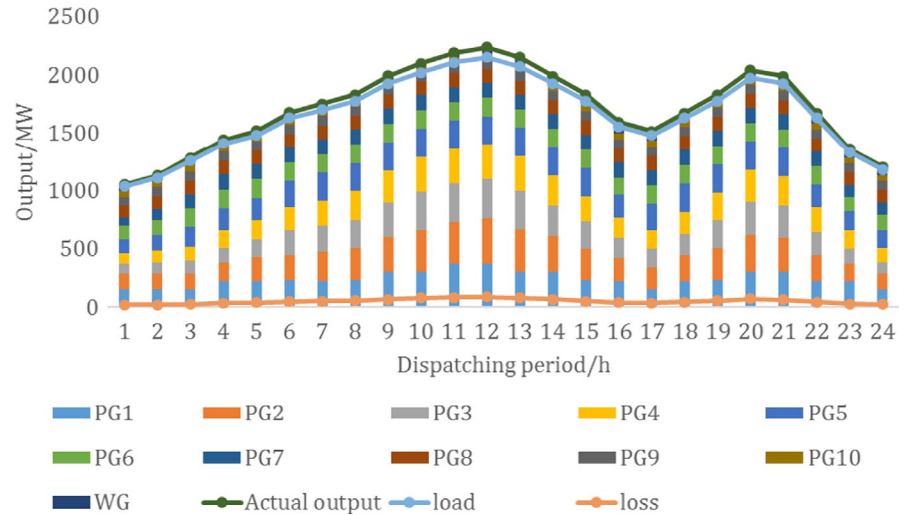


FIGURE 6 Power balance verification in case 2



The best compromise solution of EMODE in Table 4 is 2.3860×10^6 \$ and 2.6525×10^5 lb, compared with case 1, which can save 125 000\$ and reduce 33 450 lb pollution emissions. The comparison between cases 1 and 2 proves

that wind power has great economic and environmental benefits. Among all the algorithms in Table 4, the best compromise solution of EMODE is better than all other algorithms, which can also be seen vividly from Figure 5.

TABLE 5 Best compromise solution detail of the proposed algorithm in case 2

Time	Units output in each period/MW										Output/ MW	Loss/MW	Load/ MW	
	PG1	PG2	PG3	PG4	PG5	PG6	PG7	PG8	PG9	PG10				WG
1	150.26	135.10	89.29	87.27	113.92	120.54	73.92	104.26	70.87	53.33	55	1053.76	17.76	1036
2	150.23	138.29	96.37	97.77	136.69	123.21	100.38	104.50	79.29	53.86	50	1130.59	20.59	1110
3	150.51	137.83	110.91	119.76	171.55	158.16	117.01	119.17	78.95	54.92	65	1283.78	25.78	1258
4	226.41	154.71	129.64	148.67	189.51	159.56	129.75	119.11	79.93	54.93	48	1440.22	34.22	1406
5	227.00	199.63	154.30	168.17	189.76	159.01	129.60	119.81	79.43	54.04	38	1518.74	38.74	1480
6	228.35	216.15	213.47	200.11	224.51	159.89	129.66	119.60	79.78	54.91	48	1674.43	46.43	1628
7	226.25	249.70	220.82	213.64	242.89	159.97	129.96	119.95	79.94	54.61	55	1752.73	50.73	1702
8	230.01	276.28	235.80	254.06	243.00	160.00	130.00	120.00	80.00	54.99	48	1832.14	56.14	1776
9	303.21	303.31	288.51	280.43	242.19	159.30	129.85	119.83	79.84	54.25	32	1992.74	68.74	1924
10	303.75	353.23	334.74	299.99	243.00	160.00	130.00	120.00	79.99	55.00	20	2099.71	77.71	2022
11	372.69	360.89	329.22	299.87	242.89	159.87	130.00	119.93	79.89	54.84	40	2190.08	84.08	2106
12	376.07	385.32	338.13	299.98	242.92	159.99	129.97	119.94	80.00	54.99	50	2237.31	87.31	2150
13	303.94	359.70	333.62	299.99	242.99	159.99	129.99	119.99	79.99	54.99	65	2150.20	78.20	2072
14	303.36	310.44	254.66	261.71	242.97	160.00	130.00	119.85	80.00	55.00	72	1989.99	65.99	1924
15	228.68	272.31	232.85	217.62	242.99	159.99	130.00	119.99	79.99	55.00	90	1829.44	53.44	1776
16	226.83	197.38	172.53	171.07	198.58	143.61	129.65	119.68	79.18	54.87	100	1593.39	39.389	1554
17	150.75	192.36	159.06	158.51	226.92	160.00	128.15	119.71	80.00	55.00	85	1515.45	35.45	1480
18	227.42	215.32	186.41	189.38	242.78	159.54	129.96	120.00	79.70	54.80	68	1673.31	45.31	1628
19	228.66	278.09	239.60	237.25	242.98	159.87	129.96	120.00	80.00	54.97	60	1831.39	55.39	1776
20	303.10	317.25	286.15	277.36	242.97	159.97	129.97	119.95	79.978	54.96	70	2041.64	69.64	1972
21	301.09	294.69	276.67	256.30	242.46	159.88	129.98	118.52	79.98	54.98	75	1989.55	65.55	1924
22	226.48	221.64	197.32	207.45	204.19	151.64	127.22	112.61	79.55	54.00	90	1672.10	44.10	1628
23	226.08	144.52	130.00	158.66	161.66	121.04	102.43	112.34	76.42	48.11	80	1361.26	29.26	1332
24	150.00	135.00	97.91	126.52	146.73	138.89	99.00	109.68	78.14	49.46	75	1206.34	22.34	1184

Compared with MOEA/D-DE, which performs best among all compared algorithms, the suggested algorithm can save 1000\$ economic costs and reduce 4320 lb pollution emissions.

The PF shown in Figure 5 is the best among all PFs obtained by EMODE, and the HV indicator value of the present PF is 0.9302, which is the largest. The details of the best compromise solution are provided in Table 5, and the power balance is verified in Figure 5, which shows that the obtained dispatching result is feasible to solve the DEED problem with wind power.

5 | CONCLUSIONS

In this paper, an enhanced multi-objective differential evolution algorithm with multiple selection methods, which can obtain great simulation results, is proposed for the DEED problem of power system. Ramp rate constraint, valve-point effect, and spinning reserve constraint are considered for this problem, which can make the problem closer to the actual situation.

- In this work, two selection methods, NDS and SF, are used. NDS is used for dealing with the constraints of penalty function, and SF is used to judge the individual's feasibility according to the total constraint violation. The combination of the two methods makes the algorithm have better convergence.
- In case 1, 10 thermal power units are taken as dispatching objects. Compared with other algorithms, the suggested algorithm in this paper has certain advantages in solving this DEED problem and can give the best reasonable compromise solution considering both environmental and economic aspects.
- In case 2, 10 thermal power units and a wind farm are taken as dispatching objects. It is found that wind power can effectively reduce the economic cost and the pollution emission from the comparison between case 1 and case 2. Compared with other algorithms, the proposed algorithm has better results as well.
- From the simulation results of two cases, the proposed algorithm has strong ability to solve multi-objective optimization problems of DEED with constraints, and its improved selection mechanism and constraint processing technology can ensure the selected individuals feasible.

In the future work, we will focus on combining with other measures to promote the adaptation of wind power, such as energy storage and demand response. It is also hope that the suggested algorithm would be improved and used to solve other multi-objective optimization problem with constraints. At present, there are many excellent intelligent algorithms,

which have great potential in solving the DEED problem,³⁴ such as monarch butterfly optimization (MBO),³⁵ earthworm optimization algorithm (EWA),³⁶ elephant herding optimization (EHO),³⁷ and moth search (MS)³⁸ algorithm.

ACKNOWLEDGMENT

This work is supported by the Postgraduate Research & Practice Innovation Program of Jiangsu Province (KYCX20_3145).

ORCID

Yingjie Bai  <https://orcid.org/0000-0002-7867-0923>

REFERENCES

1. Mason K, Duggan J, Howley E. A multi-objective neural network trained with differential evolution for dynamic economic emission dispatch. *Int J Electr Power Energy Syst.* 2018;100:201-221.
2. Wang J-X, Duan L-Q, Yang Y-P, Pang L-P, Yang L-S. Multi-objective optimization of solar-aided coal-fired power generation system under off-design work conditions. *Energy Sci Eng.* 2019;7:379-398.
3. Zou D, Li S, Li Z, Kong X. A new global particle swarm optimization for the economic emission dispatch with or without transmission losses. *Energy Convers Manage.* 2017;139:45-70.
4. Mohammadi F, Abdi H. Solving dynamic economic emission dispatch problem by random drift particle swarm optimization considering valve-point and spinning reserve constraints. *Majlesi J Energy Manag.* 2016;5(1):1-13.
5. Kalita D, Singh S. SVM hyper-parameters optimization using quantized multi-PSO in dynamic environment. *Soft Comput.* 2020;25(24):1225-1241.
6. Yu Y-J, Chen H-K, Chen L, Chen C, Wu J. Optimal operation of the combined heat and power system equipped with power-to-heat devices for the improvement of wind energy utilization. *Energy Sci Eng.* 2019;7(5):1605-1620.
7. Xu J-X, Chang C-S, Wang X-W. Constrained multi-objective global optimization of longitudinal interconnected power system by genetic algorithm. *IEEE Proc Gen Trans Distrib.* 1996;143(5):435-446.
8. Chang C-S, Wong K-P, Fan B. Security-constrained multi-objective generation dispatch using bicriterion global optimization. *IEEE Proc Generat Trans Distrib.* 1995;142(4):406-414.
9. Basu M. Particle swarm optimization-based goal-attainment method for dynamic economic emission dispatch. *Elect Power Syst Res.* 2006;34:1015-1025.
10. Hemamalini S, Simon S. Dynamic economic dispatch using Maclaurin series based Lagrangian method. *Energy Convers Manage.* 2010;51:2212-2219.
11. Arul R, Velusami S, Ravi G. A new algorithm for combined dynamic economic emission dispatch with security constraints. *Energy.* 2015;79:496-511.
12. Li Y, Wang J, Zhao D, Li G, Chen C. A two-stage approach for combined heat and power economic emission dispatch: Combining multi-objective optimization with integrated decision making. *Energy.* 2018;162(1):237-254.
13. Rizk-Allah R-M, El-Sehiemy R-A, Wang G-G. A novel parallel hurricane optimization algorithm for secure emission/economic load dispatch solution. *Appl Soft Comput.* 2018;63:206-222.

14. Andervazh M-R, Javadi S. Emission-economic dispatch of thermal power generation units in the presence of hybrid electric vehicles and correlated wind power plants. *Generat Trans Distribut IET*. 2017;11(9):2232-2243.
15. Basu M. Dynamic economic emission dispatch using nondominated sorting genetic algorithm-II. *Electric Power Energy Syst*. 2008;30(2):140-149.
16. Guo C-X, Zhan J-P, Wu Q-H. Dynamic economic emission dispatch based on group search optimizer with multiple producers. *Electric Power Syst Res*. 2012;86:8-16.
17. Niknam T, Golestaneh F, Sadeghi M-S. θ -Multi-objective teaching-learning-based optimization for dynamic economic emission dispatch. *IEEE Syst J*. 2012;6:341-352.
18. Roy P-K, Bhui S. A multi-objective hybrid evolutionary algorithm for dynamic economic emission load dispatch. *Int Trans Elect Energy Syst*. 2016;26:49-78.
19. Huang C-L, Jao C-W, Zhang X, Yeh W-C, Jiang Y-Z. A new Method for Dynamic Economic Dispatch Problem. 2019 IEEE Congress on Evolutionary Computation. <https://doi.org/10.1109/CEC.2019.8790238>
20. Li Y, Qu B-Y, Zhu Y-S, Qiao B-H, Suganthan P-N. Dynamic economic emission dispatch based on multi-objective pigeon-inspired optimization with double disturbance. *Sci China Informat Sci*. 2019;62(7):1-3.
21. Partha B, Ponnuthurai N-S, Qu B-Y, Gehan A. Multiobjective economic-environmental power dispatch with stochastic wind-solar-small hydro power. *Energy*. 2018;150:1039-1057.
22. Wu J-K, Wu Z-S, Wu F, Mao X-M. A power balancing method of distributed generation and electric vehicle charging for minimizing operation cost of distribution systems with uncertainties. *Energy Sci Eng*. 2017;5(3):167-179.
23. Basu M. Multi-area dynamic economic emission dispatch of hydro-wind-thermal power system. *Renew Energy Focus*. 2019;28:11-35.
24. Mallipeddi R, Suganthan P-N. Ensemble of constraint handling techniques. *IEEE Trans Evol Comput*. 2010;14(4):561-579.
25. Biswas P-P, Suganthan P-N, Mallipeddi R, Amaratunga GAJ. Optimal power flow solutions using differential evolution algorithm integrated with effective constraint handling techniques. *Eng Appl Artif Intell*. 2018;68:81-100.
26. Qian S, Wu H, Xu G. An improved particle swarm optimization with clone selection principle for dynamic economic emission dispatch. *Soft Comput*. 2020;262:98-109.
27. Pandit N, Tripathi A, Tapaswi S, Pandit M. An improved bacterial foraging algorithm for combined static/dynamic environmental economic dispatch. *Appl Soft Comput*. 2012;12:3500-3513.
28. Panigrahi B-K, Pandi V-R, Das S, Das S. Multi-objective fuzzy dominance based bacterial foraging algorithm to solve economic emission dispatch. *Energy*. 2010;35(47):61-70.
29. Jiang X-W, Zhou J-Z, Wang H, Zhang Y-C. Dynamic environmental economic dispatch using multi-objective differential evolution algorithm with expanded double selection and adaptive random restart. *Elect Power Energy Syst*. 2013;49:399-407.
30. Partha B, Suganthan P-N, Qu B-Y, Gehan AJA. Multi-objective economic-environmental power dispatch with stochastic wind-solar-small hydro power. *Energy*. 2018;150(14):1039-1057.
31. Al-Betar M-A, Awadallah M-A, Khader A-T, Bolaji A, Almomani A. Economic load dispatch problems with valve-point loading using natural updated harmony search. *Neural Comput*. 2018;29(10):767-781.
32. Talbi E-H, Abaali L, Skouri R, Moudden E. Solution of economic and environmental power dispatch problem of an electrical power system using BFGS-AL algorithm. *Proc Comput Sci*. 2020;170:857-862.
33. While L, Hingston P, Barone L, Huband S. A faster algorithm for calculating hypervolume. *IEEE Trans Evol Comput*. 2006;10(1):29-38.
34. Pamulapati T, Mallipeddi R, Suganthan P-N. ISDE+—an indicator for multi and many-objective optimization. *IEEE Trans Evol Comput*. 2018;23(2):346-352.
35. Feng Y, Wang G, Deb S, Lu M, Zhao X. Monarch butterfly optimization. *Neural Comput Appl*. 2019;31:1995-2014.
36. Ghosh I, Roy P-K. Application of Earthworm Optimization Algorithm for solution of Optimal Power Flow. 2019 International Conference on Opto-Electronics and Applied Optics (Optronix); 2019. <https://doi.org/10.1109/OPTRONIX.2019.8862335>
37. Sowkarthika B, Akhilesh T, Uday P-S. Elephant herding optimization based vague association rule mining algorithm. *Int J Comput Appl*. 2017;164(5):15-23.
38. Wang G-G. Moth search algorithm: a bio-inspired metaheuristic algorithm for global optimization problems. *Memetic Comput*. 2018;10:151-164.
39. Elaiw A-M, Xia X, Shehata A-M. Hybrid DE-SQP and hybrid PSO-SQP methods for solving dynamic economic emission dispatch problem with valve-point effects. *Elect Power Syst Res*. 2013;103:192-200.
40. Zhang H-F, Yue D, Xie X-P, Hu S-L, Wen S-X. Multi-elite guide hybrid differential evolution with simulated annealing technique for dynamic economic emission dispatch. *Appl Soft Comput*. 2015;34:312-323.
41. Hu Z-J, Zhang M-L, Wang X-F, Li C, Hu M-Y. Bi-level robust dynamic economic emission dispatch considering wind power uncertainty. *Elect Power Syst Res*. 2016;135:35-47.

How to cite this article: Bai Y, Wu X, Xia A. An enhanced multi-objective differential evolution algorithm for dynamic environmental economic dispatch of power system with wind power. *Energy Sci Eng*. 2021;9:316–329. <https://doi.org/10.1002/ese3.827>

APPENDIX

TABLE A1 Fuel cost coefficient and upper and lower limits of power for thermal power units

Unit	a	b	c	d	e	$P_{G,\min}$	$P_{G,\max}$
1	786.798	38.5379	0.1524	450	0.041	150	470
2	451.3251	46.1591	0.1058	600	0.036	135	470
3	1049.9977	40.3965	0.0280	320	0.028	73	340
4	1243.5311	38.3055	0.0354	260	0.052	60	300
5	1658.5696	36.3278	0.0211	280	0.063	73	243
6	1356.6592	38.2704	0.0179	310	0.048	57	160
7	1450.7045	36.5104	0.0121	300	0.086	20	130
8	1450.7045	36.5104	0.0121	340	0.082	47	120
9	1455.6056	39.5804	0.1090	270	0.098	20	80
10	1469.4026	40.5407	0.1295	380	0.094	10	55

TABLE A2 Pollution emission coefficient and ramp rate limit of thermal power units

Unit	α	β	γ	δ	μ	U_{Ri}	D_{Ri}
1	103.3908	2.4444	0.0312	0.5035	0.0207	80	80
2	103.3908	-2.4444	0.0312	0.5035	0.0207	80	80
3	300.3910	-4.0695	0.0509	0.4968	0.0202	80	80
4	300.3910	-4.0695	0.0509	0.4968	0.0202	50	50
5	320.0006	3.8132	0.0344	0.4972	0.0200	50	50
6	320.0006	-3.8132	0.0344	0.4972	0.0200	50	50
7	330.0056	-3.9023	0.0465	0.5136	0.0214	30	30
8	330.0056	-3.9023	0.0465	0.5136	0.0214	30	30
9	350.0056	-3.9524	0.0465	0.5475	0.0234	30	30
10	360.0012	3.9864	0.0470	0.5475	0.0234	30	30